

Optimization of mass transfer-enhanced chlorine-resistant crosslinked PVA composite membranes for pervaporation desalination

Jiahua Yan^a, Zhongxiao Du^a, Zijian Yu^a, Bing Cao^a, ThiThi Mar^{a,c}, Dujian Qin^{b,*}, Rui Zhang^{a,**}

^a College of Chemical Engineering, Beijing University of Chemical Technology, Beijing 100029, China

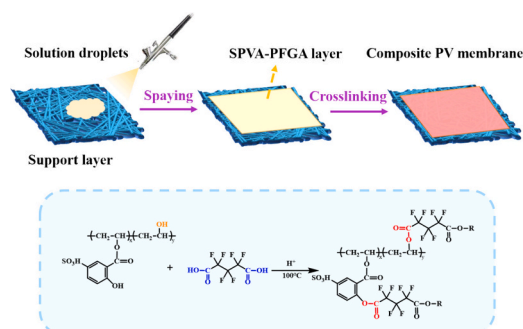
^b China SINOPEC Beijing Institute of Chemical Engineer, Yanshan Branch Institute, Beijing 102500, China

^c China National-Local Joint Engineering Research Center Of Biomass Refining and High-Quality Utilization, Changzhou 213164, China

HIGHLIGHTS

- Enhancement of the hydrophilicity of fluorine-containing crosslinked modified PVA through SSA grafting (SPVA)
- Characterization of the facilitated mass transfer structure and morphology of SPVA/PTFE desalination membrane
- Optimization of the preparation of high-flux ultra-thin separation layer SPVA-PFGA/PTFE composite membrane
- Study on the chlorine resistance of SPVA-PFGA/PTFE composite membrane
- Analysis of desalination performance of SPVA-PFGA/PTFE membrane under anti-pollution conditions

GRAPHICAL ABSTRACT



ARTICLE INFO

Keywords:

Pervaporation desalination
PVA grafting
Fluorinated crosslinker
Chlorine-resistance

ABSTRACT

Pervaporation (PV) is characterised by good hydrophilicity and antifouling properties. However, it is still unavoidable to need cleaning during long-term operation. Sodium hypochlorite (NaClO) is a commonly used purifying agent for organic pollutants, but it may cause damage to the polymer membrane. In this study, a grafting method was proposed to enhance the chlorine resistance and water permeability of membrane composite polyvinyl alcohol (PVA) pervaporation membrane. Modified PVA (SPVA) was prepared by grafting 5-sulfosalicylic acid (SSA) to improve the hydrophilicity of the membrane using the sulfonic acid group on SSA. SPVA-PFGA/PTFE composite membranes were prepared by using perfluoroglutaric acid (PFGA) as crosslinking agent to improve the chlorine resistance of the membranes by utilising the C-F chain contained therein. The water flux was $120.38 \pm 1.72 \text{ kg}/(\text{m}^2\cdot\text{h})$, which was 84.2 % higher than that before grafting, when tested at 70°C and 3.5 wt% NaCl. The chlorine resistance of SPVA-PFGA/PTFE composite membrane was tested in 2000 ppm (pH = 12) NaClO solution for 480 h, and the salt rejection remained above 99.93 %. When desalinating 20 wt% NaCl at 70°C , the water flux of SPVA-PFGA/PTFE membrane is $51.95 \pm 0.6 \text{ kg}/(\text{m}^2\cdot\text{h})$, which has the potential to treat high concentration brine.

* Corresponding author.

** Corresponding author at: College of Chemical Engineering, Beijing University of Chemical Technology, Beijing 100029, China.

E-mail addresses: qindj2017@163.com (D. Qin), zhangruil@mail.buct.edu.cn (R. Zhang).

<https://doi.org/10.1016/j.desal.2024.117872>

Received 5 March 2024; Received in revised form 7 June 2024; Accepted 24 June 2024

Available online 4 July 2024

0011-9164/© 2024 Elsevier B.V. All rights reserved, including those for text and data mining, AI training, and similar technologies.

1. Introduction

Leveraging membrane separation technology to address the challenges of water scarcity and pollution resulting from economic development and population growth has become a pivotal means in the contemporary world for resolving issues related to water resource utilization. In particular, obtaining a clean water source from seawater, brackish water, or wastewater represents a highly effective approach to addressing water resource challenges.

Pervaporation (PV) membrane, as a promising desalination technology, relies on the trans-membrane pressure difference between the two sides of the membrane as the driving force, and the effect of the salt concentration on the driving force is much smaller than that of RO [1]. Moreover, by using the renewable energy sources (such as solar, wind, etc.) or low-mass waste heat, the cost-effective desalination of PV process can reduce its energy consumption to same level with RO process [2]. Therefore, PV membrane has potential to use in the markets where RO has limitations, such as desalting treatment in high concentrated brine [3].

PVA is a widely utilized polymer material known for its advantages such as hydrophilicity, membrane-forming ability, non-toxicity [4–9]. Therefore, PVA polymer has the potential to become a water treatment membrane material that enables water molecules to preferentially undergo permeation [10–15]. However, it is precisely due to this characteristic that PVA-based membranes are easily degraded during chemical cleaning processes, especially when using NaClO solution to remove organic pollutants. [16] To enhance the chlorine resistance of membrane, many researchers devoted to introduce some chlorine resistant groups into the membrane to improve the oxidative stability of PVA, such as C-F [17–22], ester group [23,24] S=O and other functional groups. For example, Jayarani et al. [25] prepared a variety of membranes containing diester bonds, and the membrane can be operated for 7 days at 35,000 ppm NaClO solution. Cheng et al. [24] used pentaerythritol to instead piperazine to prepare a polyester nanofiltration membrane by interfacial polymerization, and the Na₂SO₄ rejection efficiency of the NF membranes was still higher than 97% after immersing in 3000 ppm NaClO for 48 h due to the stabilisation of COO⁻ in NaClO. Watanabe et al. [26] suggested that the sulfonated membranes with fluorine-containing components had good resistance to chlorine attack under harsh conditions, and the fluorinated polymers could improve the chemical inertness and long-term stability of the membranes. Therefore, introduction these functional groups into the PVA selective layer is an effective way to improve the chlorine resistance.

Our previous study reported a membranes having an improved chlorine resistance up to 768,000 ppm·h [18]. The membrane was prepared by grafting the PVA chain having 1, 3-diols unit with polystyrene-co-maleic anhydride (PSMA), and then cross-linked with the cross-linker of fluorocarbon. However, due to the hydrophobicity FS-3100 reduced the membrane hydrophilicity, the water flux was decreased to 44.5 ± 1.5 (kg/(m²·h)), which was too low to meet the requirements of PV application. Therefore, it is necessary to fabricate a membrane with high chlorine resistance and good water permeability.

The facilitated mass transfer group of sulfonic acid could promote water transport across membrane due to the hydrophilic rich domains formed a constitute continuous ion channels [10,27–30]. 5-Sulfosalicylic acid (SSA) is an aromatic compound with both sulfonic acid group, which promotes water mass transfer while ensuring the mechanical properties of the membrane. And it was a feasible method to introduce the SSA into membrane for improving the performance of the membrane.

In this study, we divided three steps to optimize the PVA composite membrane. First, the PVA was pre-oxidized with sodium periodate to remove the active 1,2 hydroxyl groups and initially improve the oxidation resistance of PVA. Subsequently, SSA and PVA were copolymerized to improve the hydrophilicity of PVA. Finally, PVA-PFGA/PTFE composite membrane was prepared by crosslinking PFGA with PVA.

2. Experimental

2.1. Chemicals

Polyvinyl alcohol (PVA-124, Mw 105,000 g mol, hydrolysis degree 98%), sodium periodate (NaIO₄, purity 99.8%), 5-sulfosalicylic acid (SSA), Bovine Serum protein (BSA), humic acid (HA) and sodium chloride (NaCl) were purchased from Aladdin Holdings-Group (Beijing, China). perfluoroglutaric acid (PFGA) was purchased from Meryer Biochemical Technology Co., LTD (Shanghai, China). PTFE was obtained from Marbridge Biomembrane Technology Co., LTD (Shanghai, China). Deionized (DI) water was obtained from a lab equipped Millipore ultrapure water system. Dimethyl sulfoxide (DMSO), Sodium hydroxide, and absolute ethyl alcohol were purchased in Tianjin Fuyu Fine Chemical Co., LTD (Tianjin, China). Concentrated sulfuric acid, sodium hypochlorite, hydrochloric acid purchased from Beijing Chemical Plant.

2.2. PVA modification

2.2.1. Oxidizing PVA hydroxyl groups

The 1,2 hydroxyl group of PVA chains was removed while the 1,3-hydroxyl group unit was kept in the PVA chain, as the oxidation method reported in ref. [17]. The pre-oxidation mechanism was shown in S1. Specially, 10 g PVA was dissolved in 90 mL DI water at 90 °C water bath. Then 5 g NaIO₄ was added to the PVA solution and stirred with 10 min at room temperature. To terminate the reaction, excess amount ethanol was poured into the mixing solution. After precipitating in 12 h, the turbid solution was filtered using ethanol for 2–3 times and vacuum dried before use.

2.2.2. Sulfonic acid grafting of modified PVA

As shown in the Fig. 1, 2 g modified PVA was added into 40 mL DMSO and stirred at 90 °C water bath for several hours. As the solution cooled to 60 °C, series amount of sulfosalicylic acid (SSA), which the molar ratio of n(COOH): n(OH) with modified PVA were 0:2, 1:2, and 2:2, were added into these solutions to react 24 h. Concentrated sulfuric acid (98%) was added in these solutions as catalyst. The solution was poured into excess ethanol and then filtered washing 2–3 times for obtaining the SSA grafted PVA (SPVA).

2.3. Fabricating the SPVA-PFGA/PTFE composite membrane

The composite membrane of SPVA-PFGA/PTFE was prepared via the spray-coating method based on a previously reported work [11]. Briefly, 2 wt% aqueous solution, which the ration of n(COOH): n(OH) in SPVA/PFGA were controlled at 1:60, 1:40, 1:20, 1:10 and 1:5, was spray-coated onto the PTFE substrate. The pH of the mixed solution was adjusted to 1 using sulfuric acid. During spraying, the nozzle diameter of air brush was selected as 0.2 mm, and the distance of spraying nozzle-membrane surface was maintained 15 cm and the air pressure was regulated at 0.3 Mpa by a mini air compressor (USTAR, UA-601G, China). Thickness of the coating SPVA-PFGA layer was controlled by depositing the spraying volumes at 70 μL/cm². After coating, the composite membrane was heated at 100 °C for 15 min to cross-link the SPVA with FA, as Fig. 2 illustrated.



Fig. 1. The reaction mechanism of SSA grafted PVA.

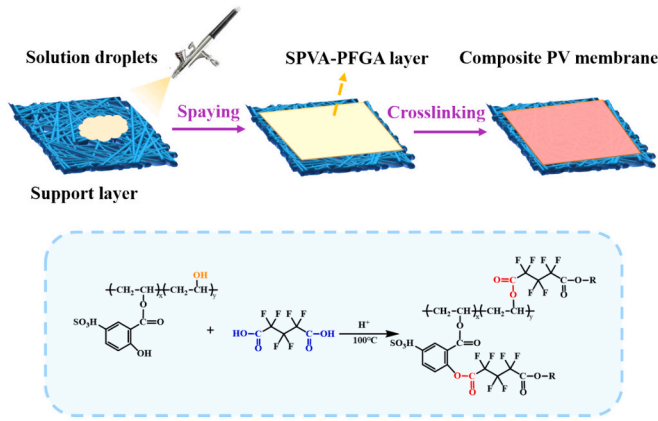


Fig. 2. Preparation process of SPVA-PFGA/PTFE composite membrane.

2.4. Physicochemical characterization of SPVA based membrane

Fourier Transform Infrared Spectroscopy (FTIR, Nicolet 560) was used to analyse the chemical structure of SPVA based membranes. The elements composition and chemical state of membranes were measured by X-ray photoelectron spectroscopy (XPS, ESCALAB 250, America). To determine the $-SO_3H$ quantity in SPVA polymer, the ion exchange capacity (IEC) was tested by titration method [28]. Specifically, 0.01 g of sample was immersed in 10 mL 0.1 mol/L NaCl solution at room temperature for 2 days. Then using the phenolphthalein as indicator, 0.02 mol/L NaOH aqueous solution was gradually titrated into the sample/NaCl solution. As the mixed solution turned red, the consuming volume of NaOH solution was recorded and then calculated the IEC by Eq. (1):

$$IEC = \frac{C_{NaOH} \times V_{NaOH}}{W_{SPVA}} \times 1000 \quad (1)$$

where IEC was Ion-exchange capability (mmol/g); C_{NaOH} was the volume (mol/L) and concentration (L) of standard sodium hydroxide; W_{SPVA} was the Weight of dry SPVA (g).

Field emission scanning electron microscope (SEM, HITACHI S-4700, Japan) was used to observe the thickness and surface of SPVA-FS membrane. All the samples were fractured in liquid nitrogen for obtaining a smooth cross-sectional morphology. Water contact angles of the membrane were measured by contact angle measuring instrument (CA, JC2000C). The CA data was the average value of five replicates at random place of each membrane. An X-ray diffractometer (XRD, Ultima IV, Rigaku, Japan) was used to analyze the crystallinity and grain size changes of the membrane at a test angle of $3\text{--}70^\circ$ and a scanning rate of $10^\circ/\text{min}$.

2.5. Pervaporation desalination test

A lab-made equipment shown in Fig. 3 was used to measure the pervaporation desalination of membranes. During the measurement, 3.5 wt% NaCl solution was circulated at membrane feed side by a peristaltic pump (JIHPUMP, China). The peristaltic pump speed was set to 400 r/min. At membrane back side, the permeation pressure was kept at 100 Pa using a vacuum pump. A liquid nitrogen cold trap was applied to draw the permeated water vapour. The collecting water was weighed to determine the water flux by Eq. (2):

$$J = \frac{\Delta M}{A \cdot t} \quad (2)$$

where J was the water flux ($\text{kg}/(\text{m}^2 \cdot \text{h})$); ΔM was the mass of producing water(kg); A was the effective area of membrane which was 3.28 cm^2 . t was the testing time(h). Salt rejection R (%) was calculated using Eq. (3):

$$R = \frac{C_f - C_p}{C_f} \times 100\% \quad (3)$$

where C_f and C_p were the salt concentrations at feed solution and penetrating solution, respectively. A conductivity meter (DDSJ-308F, Leichi, China) was used to determine the NaCl concentration of the solution. Moreover, the temperature effect on membrane performance was also studied. The membrane was tested at feed temperature of 30°C , 40°C , 50°C , 60°C , 70°C and 80°C , which was described by Arrhenius equation in Eq. (4). Taking the logarithm at both sides of Eq. (4), the function of $\ln J \sim 1/T$ was drawn and then got the activation energy of permeable water by calculating the function slope.

$$J = J_0 \exp\left(-\frac{E_j}{RT}\right) \quad (4)$$

where J was the water flux ($\text{kg}/(\text{m}^2 \cdot \text{h})$), J_0 was the pre-exponential factor, E_j (kJ/mol) was the apparent activation energy, R was the gas constant and T (K) was the feed temperature.

To better evaluate the performance of the membrane, we calculated its permeance and permeability, as detailed in the reference [31]. The permeance properties of the membrane were calculated as following Eq. (5):

$$F_{water} = \frac{\Delta M}{A \cdot t \cdot \Delta p_{water}} \quad (5)$$

where ΔM was the mass of producing water (kg); A was the effective area of membrane which was 3.28 cm^2 . t was the testing time (h); the vapor pressure on the feed side and the downstream side of the membrane (with the membrane permeate side vacuum pump pressure at 0.001 bar).

The permeability properties of the membrane were calculated as following Eq. (6):

$$P_{water} = \frac{\Delta M \cdot L}{A \cdot t \cdot \Delta p_{water}} \quad (6)$$

where L was the membrane thickness (m).

2.6. Determination of the water uptake and swelling ratio

The preparation method of SPVA-PFGA layer was referred to S1. The dried dense membrane was soaked in DI water at room temperature. As the wet membrane reached to water absorption equilibrium, the samples were taken out and wiped the water droplets on membrane surface by a tissue paper. Then the wet membrane was weighed and the samples were dried in a vacuum oven at 50°C for 12 h. Water absorption of the membrane was calculated using Eq. (7) [28]:

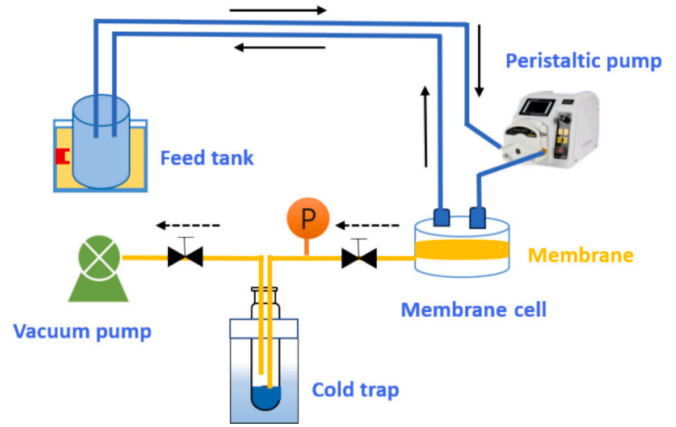


Fig. 3. Schematic diagram of pervaporation desalination.

$$WU = \frac{W_{wet} - W_{dry}}{W_{dry}} \times 100\% \quad (7)$$

where W_{wet} and W_{dry} were the mass of wet and dried membranes (g), respectively.

Rectangular samples (2 cm × 2 cm) were immersed in DI water for 48 h and swelling ratio (SR) was calculated using Eq. (8):

$$SR = \frac{L_{wet} - L_{dry}}{L_{dry}} \times 100\% \quad (8)$$

where L_{wet} and L_{dry} are the length of the water-swollen and dried membranes (cm), respectively.

2.7. Determination of the cross-linking density

The cross-linked polymer of SPVA-PFGA membrane was immersed in DI water, and the swelling behavior was described by the Flory-Rehner theory, which the cross-linking density (ν) could be calculated by Eq. (9):

$$\nu = \frac{\rho_p}{2M_c} \quad (9)$$

where ν (mol/m³) was the cross-linking density, which was the average moles number of molecular chain segments between two cross-linking sites. ρ_p (kg/m³) was the density of membrane. M_c (g/mol) was determined by Eq. (10) [32–35]:

$$M_c = -\frac{\rho_p V_s (\phi^{\frac{1}{3}} - 0.5\phi)}{(\ln(1 - \phi) + \phi + \chi\phi^2)} \quad (10)$$

where V_s (m³/mol) was the molar volume of water in gel polymer. ϕ was the volume fraction of the polymer in swelling cross-linked gel, which was calculated from Eq. (11) [34]:

$$\phi = \left[(W_d)\rho_p^{-1} \right] / \left[(W_d)\rho_p^{-1} + (W_s)\rho_s^{-1} \right] \quad (11)$$

where W_d (kg) was the mass of the cross-linked membrane, W_s (kg) was the mass of water absorbed in the swelling membrane, ρ_s (kg/m³) was the density of water. χ was the Flory Huggins interaction parameter between solvent and polymer, which was calculated using Eq. (12) [32,36]:

$$\chi = 0.44 + 0.18\phi \quad (12)$$

$$\rho_p = \frac{A}{A - B} + \rho_0 + \rho_L + \rho_A \quad (13)$$

where A (kg) was the dry weight of SPVA-PFGA membrane, B (kg) was the mass of wet membrane, ρ_0 (kg/m³) was the density of DI water, and ρ_L (kg/m³) was the density of air.

2.8. Evaluation of the chlorine resistance

To evaluate the oxidation resistance of the prepared SPVA-PFGA/PTFE membranes, 3.5 wt% NaCl was used as the feed salt solution, and the permeability flux and desalination rate before and after oxidation exposure were calculated. The salt solution was run for 1 h to establish the initial flux before testing for oxidation resistance. The oxidation resistance experiments were carried out by soaking the membranes in 2000 ppm NaClO solutions that regulated with various pH value (4, 7, 12). After immersing a period time of 48 h, the membrane was taken out and washed carefully with DI water for PV testing. The changes in PV desalination properties and chemical structure of the SPVA-FA membranes over the soaking time were monitored by PV device and FTIR, respectively. The total free chlorine exposure of the PV composite membrane was calculated by Eq. (14) [18,37]:

$$C \cdot t(\text{ppm} \cdot \text{h}) = \int C dt \quad (14)$$

where C (ppm) was the concentration of sodium hypochlorite; t (h) was the immersion time in sodium hypochlorite.

2.8.1. Membrane fouling and washing experiments

The membrane was firstly stabilized by PV tests in 3.5 wt% NaCl aqueous solution for 1 h, and denoted the water flux as J_{W1} . Subsequently, the membrane was exposed to 3.5 wt% NaCl+1 wt% BSA solutions for continuous contamination reaching to 10 h. Then the membrane was immersed for 30 min using NaOH (pH = 12). After that, the membrane was tested using 3.5 wt% NaCl solution, which the water flux was noted as J_{W2} . The flux recovery ratio (FRR) was calculated using Eq. (15). Subsequently, the second and third cycles were conducted following the aforementioned steps, using NaOH + SDS and NaClO (pH = 12) as cleaning agents, respectively, to compare the cleaning effectiveness of different agents. The contamination solution of 3.5 wt% NaCl+1 wt% HA was also carried out as the same procedure.

$$FRR = \frac{J_{W2}}{J_{W1}} \quad (15)$$

where J_{W1} (kg/(m²·h)) was the water flux before fouling, J_{W2} (kg/(m²·h)) was the water flux after cleaning.

3. Results and discussion

3.1. Characterization of the SPVA

FTIR in Fig. 4(a) was the spectra of PVA, SSA and SPVA. For PVA, a wavenumber in 1720 cm⁻¹ appeared, which represented the characteristic peak of C=O. This was reasoned from the vinyl acetate that had not been hydrolyzed [17]. After grafting SSA, the intensity of C=O in modified PVA (SPVA) was enhanced and the bands located at 1050 cm⁻¹ and 1088 cm⁻¹ were attributed to the stretching vibration of S-O, respectively, which proved the existence of sulfonic groups [28]. This was because the SSA had reacted with the PVA by esterification reaction. XPS spectrum also demonstrated this result. Fig. 4(c) shown that no characteristic peak of S at binding energy between 155–180 eV [38] was observed for the PVA (n(COOH): n(OH) = 0:2) While as the n(COOH): n(OH) increased to 2:2, the signal of S was detected. More specifically, by analysing the C1s XPS spectrum in Fig. 2(d)–(f), the peak intensity of C-S peak increased gradually with the increased amount of SSA (SPVA (0:2) to SPVA (2:2)). This result indicated the increased graft proportion of SSA. The content of sulfonic acid group can be determined by using IEC standard method. Fig. 4(b) shown that there was an improved IEC data as the SSA content increment. The highest IEC of 0.72 mmol/g was observed when n(COOH): n(OH) = 2:2, which suggested the highest grafting efficiency for the SPVA.

3.2. Effect of SSA grafting amount on PV desalination performance

The SPVA with changed SSA grafting ratio was mixed with certain amount of cross-linking agent PFGA and then cross-linked on PTFE substrate. Fig. 5(a) shown the surface and cross-sectional morphologies of PVA, and SPVA (1:2, 2:2) on PTFE. The thickness of these layers was about 6 μm. PV desalination performance was shown in Fig. 5(b). It was observed that all the membranes had a NaCl rejection above 99.9 %. This result indicated the prepared membrane was defect-free, which could meet the desalting application. However, the water flux of these membranes varied significantly with the improvement of SSA grafting ratio. The water flux improved to 120.38 ± 1.72 (kg/(m²·h)) from 65.35 ± 2.62 (kg/(m²·h)) with the n(COOH): n(OH) ratio increased from 0:2 to 2:2.

Two reasons could explain this change: 1) the SSA grafted membrane

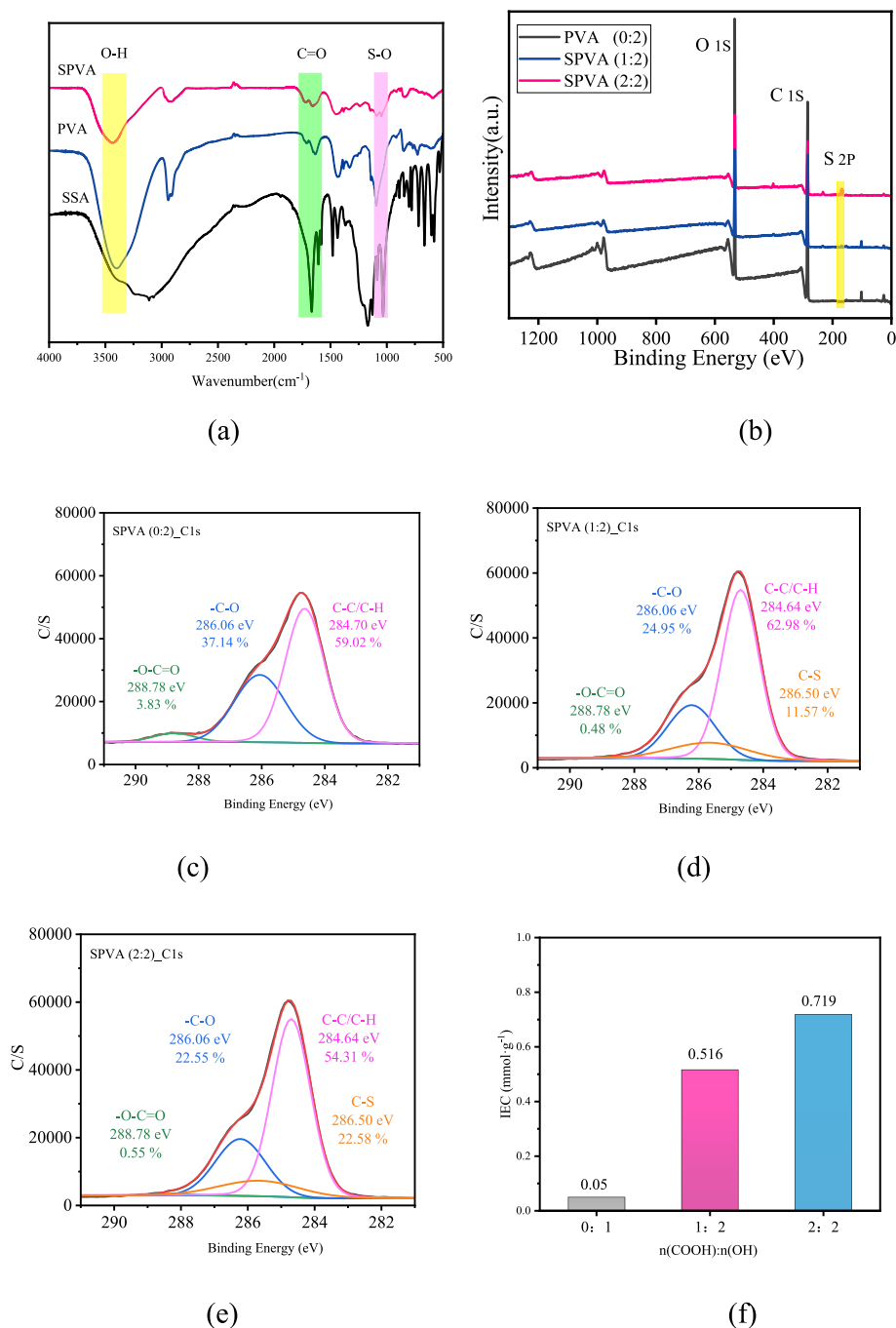
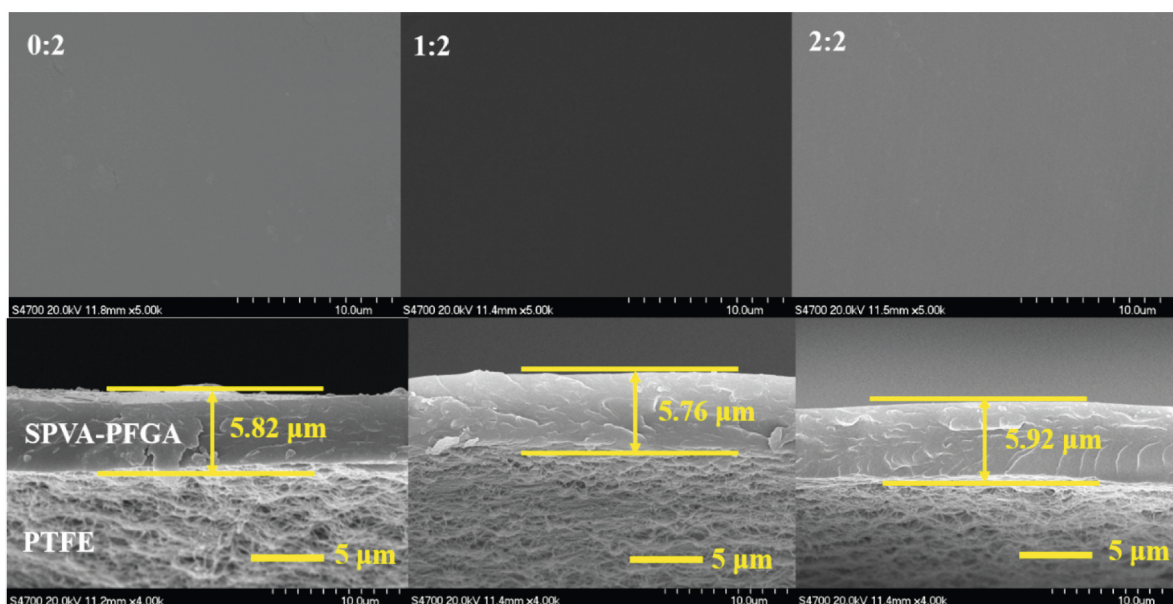


Fig. 4. (a) FTIR spectra of SPVA, PVA and SSA; (b) XPS spectra of PVA; XPS spectra of (c) PVA (0:2), (d) SPVA (1:2) and (d) SPVA (2:2) membranes; (f) IEC of SPVA with different grafting proportions.

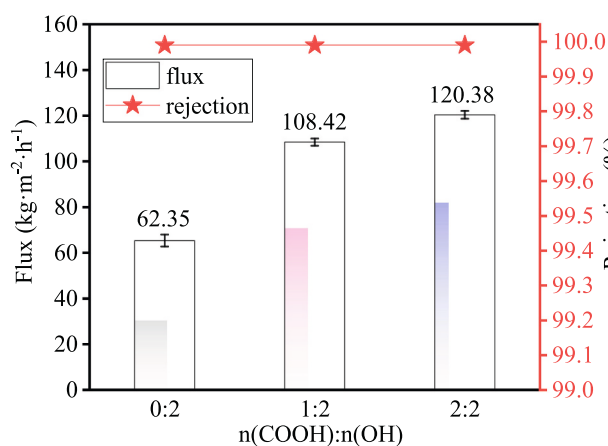
had strong water absorption capacity, providing higher water content, and thus led to a higher driving force for water molecule diffuse through the membrane. Fig. 5(d) confirmed the development trend of water absorption and swelling degree for these membranes. The initial PVA exhibited the lowest water absorption (70.41 %) and swelling ability (36.67 %), while the highest water absorption (225.0 %) and swelling (80.67 %) were observed for SPVA (2:2). 2) sulfonic acid groups had strong water-absorbing ability, which was a facilitated mass transfer factor for water. The water accumulated near the sulfonic acid group and then passed across the membrane rapidly [10,29].

3.3. Cross-linking density influence on PV desalination property

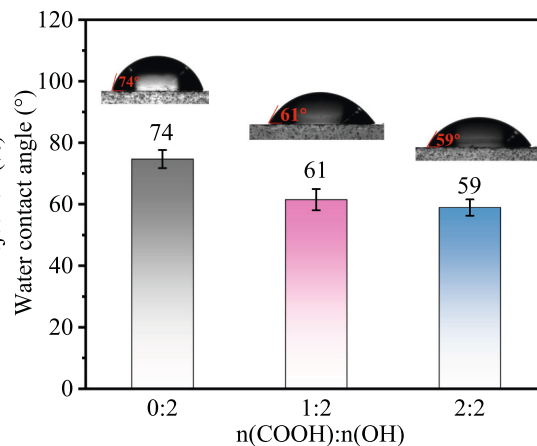
The effect of SPVA/PFGA membranes cross-linking density on PV desalination property was explored. Fig. 6(a) was the cross-linking degree of SPVA/FA membrane. It was found the cross-linking degree of these membranes increased from 403 ± 21.72 (mol·m⁻³) to 687 ± 32.62 (mol·m⁻³), as the n(COOH): n(OH) (PFGA: SPVA) increased from 1:60 to 1:10. Cross-linking also changed the crystallinity of the membrane, expanding the amorphous part of the membrane and facilitating the diffusion of water molecules [17]. Therefore, the water flux was of these membranes continuously improved from 58.08 ± 1.64 kg/(m²·h) to 120.38 ± 1.72 kg/(m²·h) following the n(COOH): n(OH) rose from 1:60 to 1:10. However, when the n(COOH): n(OH) (PFGA: SPVA) increased to



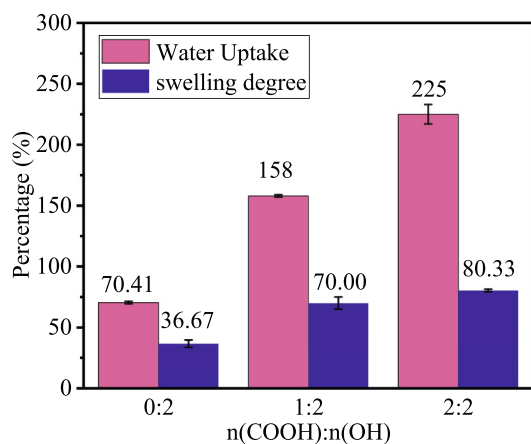
(a)



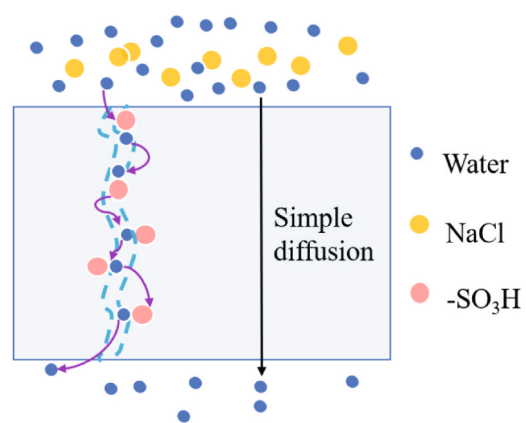
(b)



(c)



(d)



(e)

Fig. 5. (a) SEM images of cross-section morphology of 0:2, 1:2, 2:2 SPVA-PFGA/PTFE membranes; (b) the water flux and salt rejection of PV composite membranes with different grafting ratio during pervaporation desalination experiments at 70 °C and 3.5 wt% NaCl; contact angle (c) and water absorption and swelling degree (d) of PV composite membranes with different grafting ratio; (e) SPVA-FA selective layer water transport mechanism.

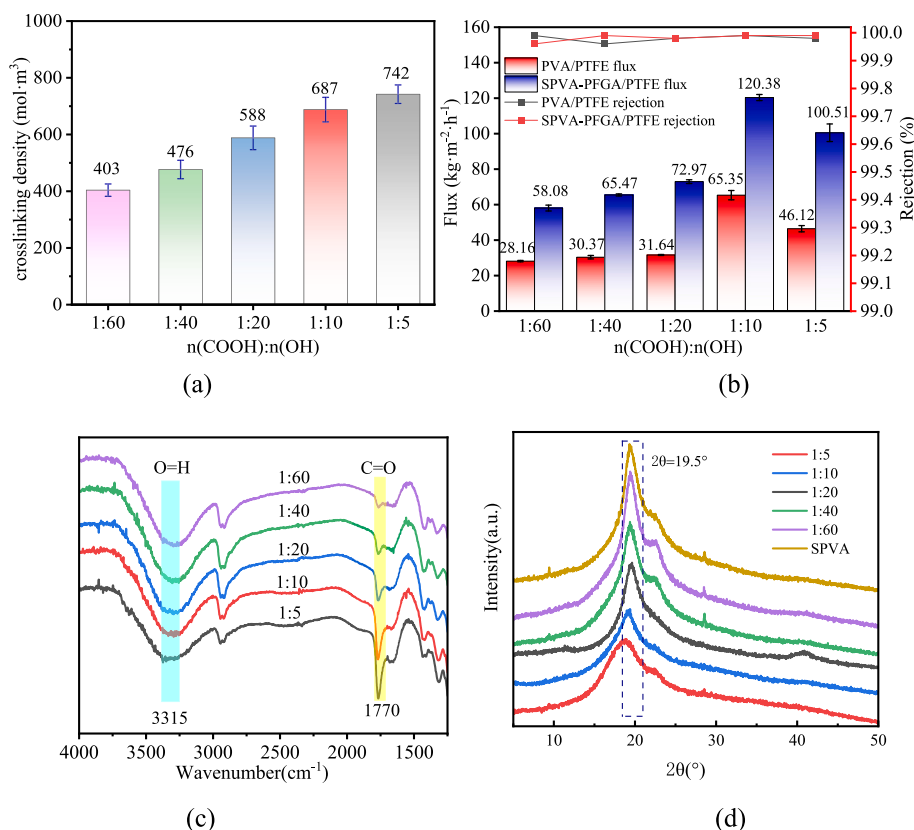


Fig. 6. (a) Crosslink density of grafted PVA layers as a function of crosslinking agent (PFGA) additions; (b) the pervaporation desalination properties of all SPVA-PFGA/PTFE composite membranes at 70 °C; (c) FTIR spectra of SPVA-PFGA membranes with various crosslinking ratios; (d) XRD spectra of SPVA and SPVA-PFGA membrane.

1:5, the water flux of membranes decreased to $100.51 \pm 4.95 \text{ kg}/(\text{m}^2 \cdot \text{h})$. This was mainly due to the excessive cross-linking for the SPVA/PFGA membranes.

Fig. 6(c) shown the FTIR spectra for membranes with different addition of PFGA. Following the increment of PFGA, the C=O peak at 1770 cm^{-1} was developed to deeper, and then the growing tendency became stable when the $n(\text{COOH}) : n(\text{OH})$ reached to 1:5. This signified sufficient -COOH in PFGA had reacted with the OH in SPVA and thus the signal of C=O peak reached to saturation. The over cross-linked structure of PVA restricted the chain movement, and the overall flexibility of the polymer decreased, which directly affected the transfer to water, and thus leads to a decrease in the flux [18]. In addition, the hydrophobicity of PFGA led to a decrease in the hydrophilicity of the SPVA-PFGA polymer, which resulted in a decrease in membrane water flux at high PFGA concentration.

XRD tests were conducted on the membranes with different ratios of crosslinking agents. As shown in Fig. 6(d), $2\theta = 19.5^\circ$ was the typical crystallization peak of polymer SPVA, which was significantly lower than before crosslinking, indicating that the amorphous part of polymer PVA expanded after crosslinking. This will facilitate the migration of more PVA molecular chain fragments and promote the diffusion of water [17].

3.4. Effect of operation conditions and performance sustainability

Fig. 7(a) demonstrated the desalting performance of the SPVA-PFGA/PTFE($n(\text{COOH}) : n(\text{OH}) = 1:10$) membrane at varied feed temperature. It was observed that all the membranes kept NaCl rejection above 99.98 % from 30 °C to 80 °C. But the water flux of membrane increased significantly with the improvement of feed temperature. When the operated temperature rose to 80 °C, a high water flux of

$136.89 \pm 2.72 \text{ kg}/(\text{m}^2 \cdot \text{h})$ was achieved, which was increased by 3.1 times comparing than that performance obtained at feed temperature of 30 °C. This was because the increased feed temperature made higher driving force of water vapor partial pressure difference between the feed side and the permeating side, therefore, allowed more water to spread through the membrane [18]. On the other hand, the improved temperature was conducive to increase the mobility of the polymer chains, making it easier for water to diffuse across the membrane [39]. The temperature effect on desalination performance could be described by Arrhenius equation. After calculation from the slope of Arrhenius plot in Fig. 7(b), the E_j was to be 25.67 kJ/mol. In addition, the activation energies were compared with those of other PV membranes, with more details listed in Table S3.

It can be observed that SPVA-PFGA/PTFE composite membranes outperform most other materials used for PV desalination in terms of water flux in the temperature range of 30–80 °C (Fig. 7(c)). The membranes have very great water permeability, excellent salt rejection properties and strong interfacial strength, which make them an important application area for PV desalination.

Salt concentration also affected membrane performance. Fig. 7(d) shown the performance of membrane operating as the NaCl concentration increased from 0 wt% to 20 wt%. The water flux decreased clearly with the increased NaCl concentration. This could be easy understanding that the high feed concentration decreased the water vapour pressure and intensified the concentration polarization at membrane feed side [40]. Nevertheless, even at 20 wt% NaCl concentration, the membranes still had a flux of $51.95 \pm 0.6 \text{ kg}/(\text{m}^2 \cdot \text{h})$ and good salt rejection above 99.98 %. This membrane had acceptable water flux, salt rejection properties, which suggested a promising prospect for PV desalination in treating high-concentration saline water. Compared to other membranes, SPVA-PFGA/PTFE shows good permeance and permeability, as

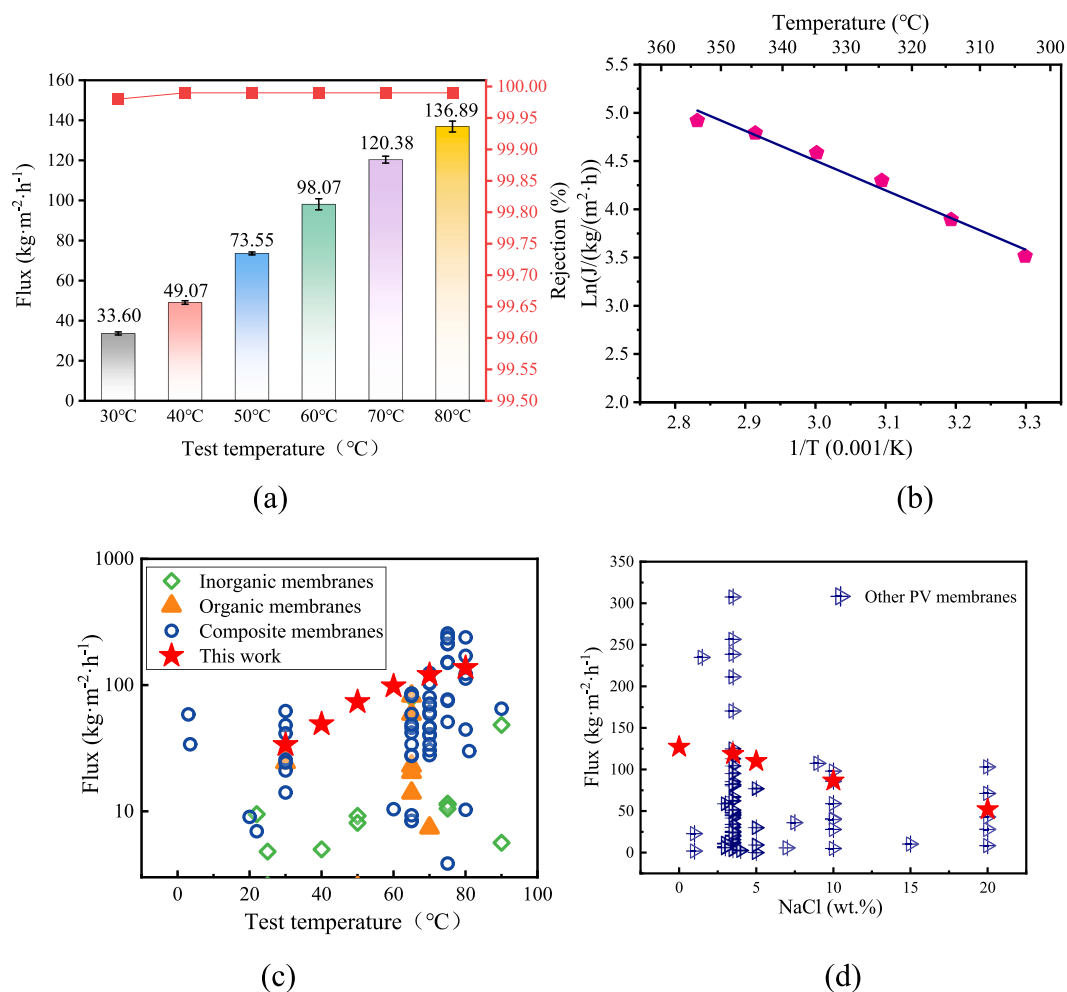


Fig. 7. (a) Salt rejection and water flux of SPVA-PFGA/PTFE at different test temperatures (3.5 wt% NaCl solution); (b) the water flux Arrhenius plot of SPVA-PFGA/PTFE composite membrane at different temperatures; (c) comparison of the PV desalination performance of this work with previously reported results in the literature; (d) Comparison of water fluxes with other PV membranes at different salt concentrations [13,15,17,28,29,41–67] (Table S2).

shown in Table 1.

3.5. Chlorine resistance

The beginning of reduction trend in salt rejections taken as a evidence that the chlorine had damaged the SPVA-PFGA separation layer. Fig. 8(a) shown the steady running time of the membranes soaking in NaClO solutions (pH = 12) reached to 480 h, corresponding to the chlorine and recorded as the oxidation resistance of 960,000 ppm·h. Comparing with the oxidation resistance property reported by other literature in Fig. 8(e), the chlorine resistance ability was the highest level. S1 S4 lists more details. Besides that, the membrane soaking in NaClO solutions (pH = 4, 7) were 192 h and 216 h, corresponding to the chlorine resistance of 384,000 ppm·h and 432,000 ppm·h, respectively.

Table 1
The performance comparison between our membrane with literature-reported work.

Membrane	Thickness	Feed temp. (°C)	Salt conc. (wt%)	Flux (kg/m ² ·h)	Permeance (kg/m ² ·h·bar)	Permeability (kg·m/m ² ·h·bar) × 10 ⁻⁴	Ref.
SPVA-PFGA/PTFE	6.12 μm	70	3.5	120.38	397.29	24.31	This work
PVA/PAN nanofiber	0.73 μm	75	3.5	211.37	569.55	4.16	[15]
PVA/ZIF-8/PTFE	1.18 μm	80	3.5	307.58	674.37	7.96	[31]
(CTA/CNCs)	6	70	3	11.67	37.76	2.26	[66]
PVA/PVDF	0.88 μm	85	3.5	120.0	215.32	1.89	[68]
PVA/PSF	0.61 μm	70	3.5	124.8	416.28	2.54	[12]
Cellulose triacetate/LUDOX-SiO ₂	10	70	3	6.1	19.74	1.97	[67]

Clearly, the membrane treated in alkaline NaClO solutions had better chlorine resistance performance. This because of there was a higher oxidation potential in neutral and acidic conditions for HClO compared with ClO⁻ in alkaline environment, and thus the oxydic capacity of HClO exceeded that of ClO⁻ [18]. Therefore, it was recommended to clean the polluted membrane in alkaline NaClO solution for reducing membrane damage as much as possible resistance time.

The water flux increased and then decreased with longer soaking time. The water flux increased by 42 % after 96 h of NaClO soaking. As the hydrolysis of the membrane by sodium hypochlorite dominated the hydrolysis of the membrane, the carboxyl groups increased and the peaks of C=O at 1700 cm⁻¹ became stronger in the FTIR of Fig. 8(b, c, and d), which made the membrane more hydrophilic. In the event of a minor reduction in cross-linking, the membrane's salt rejection and

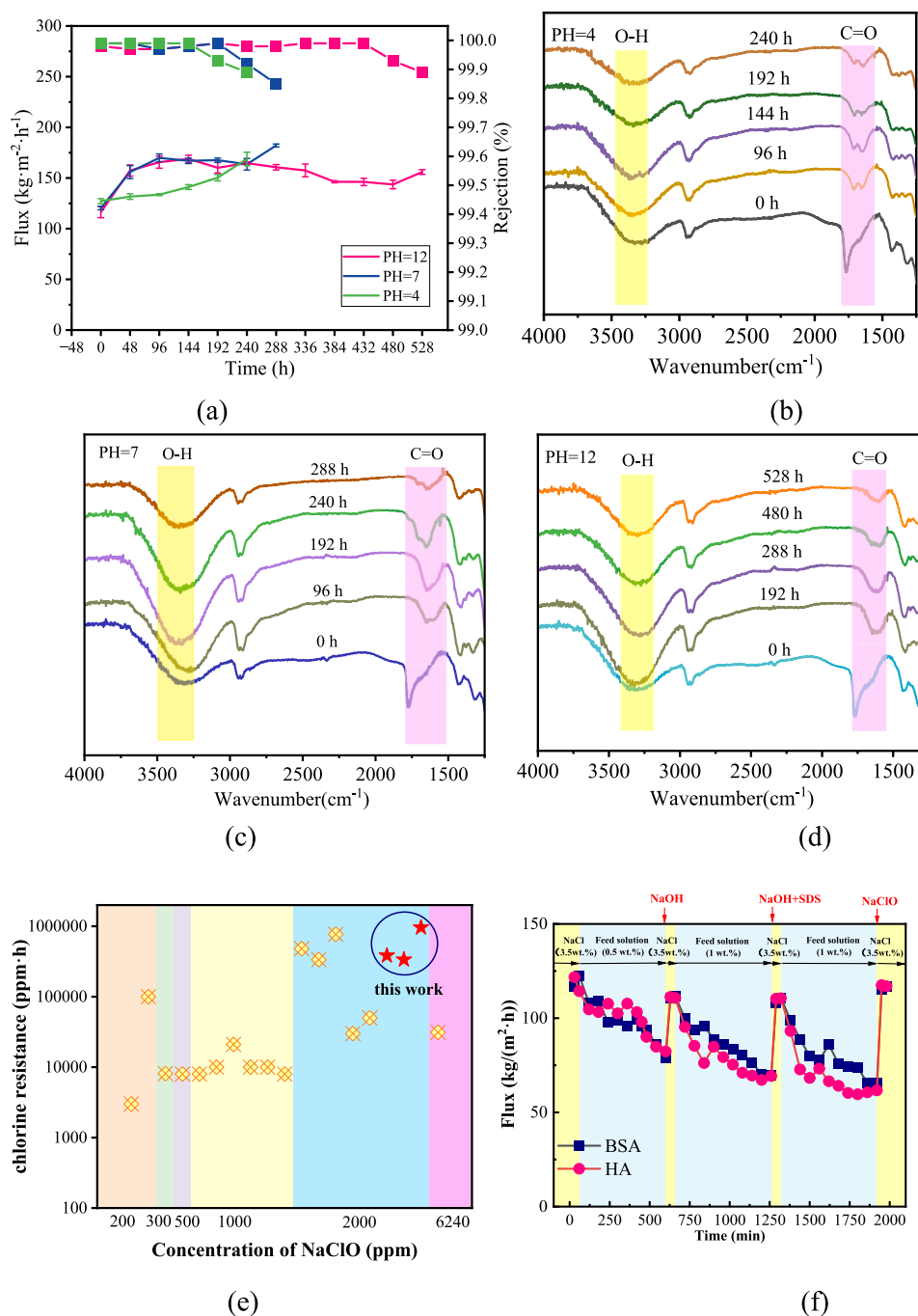


Fig. 8. (a) Oxidation resistance test at different pH values (2000 ppm NaClO); FTIR changes of composite membranes at pH = 4 (b), pH = 7 (c) and pH = 12 (d); (e) Oxidation resistance compared with other membranes [17,18,70–80]; (f) Contamination - cleaning test. The contaminated membrane was cleaned with NaOH (pH = 12), NaOH + SDS (0.03 %) and 500 ppm NaClO (pH = 12), respectively.

permeability were improved, leading to an increase in water flux through the membrane. With further increase in immersion time, the water flux started to decrease possibly due to the increase in free volume of the hydrolysed polymer, and the loose structure of the polymer collapsed more easily under pressure. When immersed for 480 h, the 1700 cm^{-1} peak became broader and weaker, while the intensity of the broad peak between 3000 cm^{-1} – 3300 cm^{-1} decreased significantly, indicating that the hydroxyl group on the PVA was oxidised to carboxylic acid by the residual chlorine, which indicated that at this time, the decomposition of the PVA chain occurred in the residual chlorine solution, and the integrity of the membrane was damaged, with a significant decrease in the salt cut-off chlorine, and a significant increase in

the water flux.

We selected humic acid (HA) and bovine serum albumin (BSA) as organic pollutants in the feed solution, and NaOH (pH = 12), NaOH + SDS, and NaClO (pH = 12) aqueous solutions as cleaning agents for membrane washing [18]. As shown in Fig. 8(f), the water flux decreased sharply after adding HA or BSA to the feed solution, followed by a gradual decline and stabilization. This indicates that the membrane surface was completely covered by a cake layer formed by organic pollutants [69]. In the first cycle, after static soaking with water for 30 min, the water flux recovered to $111.34 \pm 0.93\text{ (kg}/(\text{m}^2\cdot\text{h}))$ and $118 \pm 5.26\text{ (kg}/(\text{m}^2\cdot\text{h}))$. In the subsequent 10 h fouling test, the second cycle used NaOH + SDS solution for membrane cleaning, following the same

procedure as the first cycle. It was observed that the membrane flux was significantly higher after cleaning. This is because SDS, as a surfactant, effectively removes organic molecules. In the third cycle, NaClO solution was used, resulting in the highest flux recovery rate among the three cleaning methods. This demonstrates that NaClO is the most effective chemical for removing organic fouling, as HA and BSA are oxidized into smaller molecules. Membrane fouling and cleaning experiments demonstrated that our developed PV composite membranes exhibit over 90 % water flux recovery following chemical cleaning (Fig. S4).

4. Conclusion

In this study, we developed a PVA-based PV membrane with excellent chlorine resistance. The oxidation resistance of PVA was improved by removing 1,2-diol from PVA, SSA grafting and PFGA cross-linking. Grafting of SSA and introduction of sulfonic acid groups resulted in decreased crystallinity and increased hydrophilicity of PVA, which improved the intrinsic water transport properties of cross-linked SPVA-PFGA polymer. The water flux increased from 65.35 ± 2.62 (kg/(m²·h)) to 120.38 ± 1.72 (kg/(m²·h)) in a pervaporation desalination experiment with 3.5 wt% NaCl at 70 °C, which is a 94.54 % increase in water flux, while the high salt rejection was maintained at more than 99.95 %. The SPVA-PFGA/PTFE composite membranes exhibited excellent chlorine resistance at different pH values (pH = 4, 7, 12, NaClO = 2000 ppm). The modified composite membrane had a salt rejection of 99.93 % at pH = 12 for 480 h continuously and a chlorine resistance of 960,000 ppm·h. Membrane fouling and cleaning experiments demonstrated that our developed PV composite membranes exhibit over 90 % water flux recovery following chemical cleaning. This significant achievement underscores the membrane's exceptional oxidative stability and regenerative capacity. By enhancing the chlorine stability and water permeability of PVA membranes, the PV composite membrane not only expands its potential for high-demand water treatment applications but also offers an innovative solution to the challenges of industrial membrane fouling and lifespan extension. This improvement is poised to drive the future development of oxidation-resistant membranes, providing reliable and efficient water treatment technology for industrial applications, suggesting broader applicability and greater economic benefits.

Declaration of competing interest

The authors declare that they have no known competing financial interests or personal relationships that could have appeared to influence the work reported in this paper.

Data availability

Data will be made available on request.

Acknowledgments

The first author thanks Dr. Dujian Qin from SINOPEC Beijing Institute of Chemical Engineer, Yanshan Branch Institute for his assistance in revising the article. The first author thanks Mr. Rui Zhang for the guidance of the experiment. We also gratefully acknowledge the support from the NERC204 project (Changzhou Key Laboratory of Biomass Green, Safe & High Value Utilization), which significantly contributed to the success of this research.

Appendix A. Supplementary data

Supplementary data to this article can be found online at <https://doi.org/10.1016/j.desal.2024.117872>.

References

- [1] T. Eljaddi, D.L.M. Mendez, E. Favre, D. Roizard, Development of new pervaporation composite membranes for desalination: Theoretical and experimental investigations, *Desalination*, 507, 2021.
- [2] I. Prihatiningtyas, A.-H.A.H. Al-Kebsi, Y. Hartanto, T.M. Zewdie, B. Van der Bruggen, Techno-economic assessment of pervaporation desalination of hypersaline water, *Desalination*, 527, 2022.
- [3] Z. Xie, D. Ng, M. Hoang, J. Zhang, S. Gray, Study of Hybrid PVA/MA/TEOS Pervaporation Membrane and Evaluation of Energy Requirement for Desalination by Pervaporation, *International Journal of Environmental Research and Public Health*, 15, 2018.
- [4] L.L. Xia, C.L. Li, Y. Wang, In-situ crosslinked PVA/organosilica hybrid membranes for pervaporation separations, *J. Membr. Sci.* 498 (2016) 263–275.
- [5] C.K. Yeom, K.-H. Lee, Characterization of sodium alginate membrane crosslinked with glutaraldehyde in pervaporation separation, *J. Appl. Polym. Sci.* 67 (1998) 209–219.
- [6] T. Hirai, Y. Asada, T. Suzuki, S. Hayashi, M. Nambu, Studies on elastic hydrogel membrane. I. Effect of preparation conditions on the membrane performance, *J. Appl. Polym. Sci.* 38 (1989) 491–502.
- [7] N.A. Ibrahim, M.H. Abo-Shosha, Preparation and characterization of carboxylic cation exchange resins from the reaction of poly(vinyl alcohol) with melamine-formaldehyde and some hydroxy acids, *Angew. Makromol. Chem.* 210 (1993) 7–20.
- [8] K. Yamaura, M. Itoh, T. Tanigami, S. Matsuzawa, Properties of gels obtained by freezing/thawing of poly(vinyl alcohol)/water/dimethyl sulfoxide solutions, *J. Appl. Polym. Sci.* 37 (1989) 2709–2718.
- [9] W.-I. Cha, S.-H. Hyon, Y. Ikada, Transparent poly(vinyl alcohol) hydrogel with high water content and high strength, *Die Makromolekulare Chemie* 193 (1992) 1913–1925.
- [10] W.S. Mengyu Yan, Na Li, Yin Chen, Zongli Xie, Meixin Liu, Jinjia Wei Construction of high performance sulfonated aromatic block copolymer/ PTFE composite membrane for pervaporation desalination, *J. Membr. Sci.*, 8 (2023) 121753.
- [11] J. Meng, C.H. Lau, Y. Xue, R. Zhang, B. Cao, P. Li, Compatibilizing hydrophilic and hydrophobic polymers via spray coating for desalination, *J. Mater. Chem. A* 8 (2020) 8462–8468.
- [12] D. Qin, H. Liu, T. Xiong, J. Wang, R. Zhang, B. Cao, P. Li, Enhancing the property of composite pervaporation desalination membrane by fabricating a less resistance substrate with porous but skinless surface structure, *Desalination*, 525, 2022.
- [13] A. Selim, A.J. Toth, E. Haaz, D. Fozer, A. Szanyi, N. Hegyesi, P. Mizsey, Preparation and characterization of PVA/GA/Laponite membranes to enhance pervaporation desalination performance, *Sep. Purif. Technol.* 221 (2019) 201–210.
- [14] S. Zachariah, Y.-L. Liu, Surface engineering through biomimicked structures and deprotonation of poly(vinyl alcohol) membranes for pervaporation desalination, *Journal of Membrane Science*, 637, 2021.
- [15] Y.L. Xue, J. Huang, C.H. Lau, B. Cao, P. Li, Tailoring the molecular structure of crosslinked polymers for pervaporation desalination, *Nat. Commun.* 11 (2020) 1461.
- [16] B. Ye, Y. Li, Z. Chen, Q.-Y. Wu, W.-L. Wang, T. Wang, H.-Y. Hu, Degradation of polyvinyl alcohol (PVA) by UV/chlorine oxidation: Radical roles, influencing factors, and degradation pathway, *Water Res.* 124 (2017) 381–387.
- [17] P. Zhao, Y. Xue, R. Zhang, B. Cao, P. Li, Fabrication of pervaporation desalination membranes with excellent chemical resistance for chemical washing, *Journal of Membrane Science*, 611, 2020.
- [18] Z. Pengbo, M. Junquan, Z. Rui, C. Bing, L. Pei, Molecular design of chlorine-resistant polymer for pervaporation desalination, *Separation and Purification Technology*, 268, 2021.
- [19] K.-S. Lee, M.-H. Jeong, J.-P. Lee, J.-S. Lee, End-Group Cross-Linked Poly(arylene ether) for Proton Exchange Membranes, *Macromolecules* 42 (2009) 584–590.
- [20] Y.-J. Kim, K.-S. Lee, M.-H. Jeong, J.-S. Lee, Highly chlorine-resistant end-group crosslinked sulfonated-fluorinated poly(arylene ether) for reverse osmosis membrane, *J. Membr. Sci.* 378 (2011) 512–519.
- [21] S. Bonyadi, T.-S. Chung, Highly porous and macrovoid-free PVDF hollow fiber membranes for membrane distillation by a solvent-dope solution co-extrusion approach, *J. Membr. Sci.* 331 (2009) 66–74.
- [22] S.-M. Xue, C.-H. Ji, Z.-L. Xu, Y.-J. Tang, R.-H. Li, Chlorine resistant TFN nanofiltration membrane incorporated with octadecylamine-grafted GO and fluorine-containing monomer, *J. Membr. Sci.* 545 (2018) 185–195.
- [23] P.R.R. M.M. Jayarani, S.S. Kulkarni, U.K. Kharul Synthesis of model diamide, diester and esteramide adducts and studies on their chlorine tolerance, *Desalination*, 130 (2000) 1–16.
- [24] J. Cheng, W. Shi, L. Zhang, R. Zhang, A novel polyester composite nanofiltration membrane formed by interfacial polymerization of pentaerythritol (PE) and trimesoyl chloride (TMC), *Appl. Surf. Sci.* 416 (2017) 152–159.
- [25] S.S.K. M.M. Jayarani, Thin-film composite poly(esteramide)-based membranes, *Desalination* 130 (2000) 17–30.
- [26] R. Verbeke, V. Gómez, I.F.J. Vankelecom, Chlorine-resistance of reverse osmosis (RO) polyamide membranes, *Prog. Polym. Sci.* 72 (2017) 1–15.
- [27] J.-E. Yang, J.-S. Lee, Selective modification of block copolymers as proton exchange membranes, *Electrochim. Acta* 50 (2004) 617–620.
- [28] M. Yan, Y. Lu, N. Li, F. Zeng, Q. Wang, H. Bai, Z. Xie, Hyperbranch-Crosslinked S-SEBS Block Copolymer Membranes for Desalination by Pervaporation, *Membranes (Basel)*, 10, 2020.
- [29] B. Liang, Q. Li, B. Cao, P. Li, Water permeance, permeability and desalination properties of the sulfonic acid functionalized composite pervaporation membranes, *Desalination* 433 (2018) 132–140.

- [30] G. Yang, Z. Xie, M. Cran, D. Ng, C.D. Easton, M. Ding, H. Xu, S. Gray, Functionalizing graphene oxide framework membranes with sulfonic acid groups for superior aqueous mixture separation, *J. Mater. Chem. A* 7 (2019) 19682–19690.
- [31] D. Qin, H. Liu, J. Yan, Z. Yu, Z. Du, B. Cao, R. Zhang, Large-scale preparation of UV photo-crosslinked composite membrane with high pervaporation desalination properties and excellent fouling resistance, *Journal of Membrane Science*, 691, 2024.
- [32] A.I.A. A.R.R. Menon, C.K.S. Pillai, N.M. Mathew, S.S. Bhagawan Processability characteristics and physico-mechanical properties of natural rubber modified with cashewnut shell liquid and cashewnut shell liquid–formaldehyde resin, *European Polymer Journal* 38 (2002) 163–168.
- [33] L. Deng, Y. Xue, J. Yan, C.H. Lau, B. Cao, P. Li, Oxidative crosslinking of copolyimides at sub-Tg temperatures to enhance resistance against CO₂-induced plasticization, *J. Membr. Sci.* 583 (2019) 40–48.
- [34] P. Garg, R.P. Singh, V. Choudhary, Selective polydimethylsiloxane/polyimide blended IPN pervaporation membrane for methanol/toluene azeotrope separation, *Sep. Purif. Technol.* 76 (2011) 407–418.
- [35] P.J. Flory, J. Rehner Jr., Statistical Mechanics of Cross-Linked Polymer Networks II. Swelling, *J. Chem. Phys.* 11 (2004) 521–526.
- [36] S.-B. Lin, C.-H. Yuan, A.-R. Ke, Z.-L. Quan, Electrical response characterization of PVA-P(AA/AMPS) IPN hydrogels in aqueous Na₂SO₄ solution, *Sens. Actuators B* 134 (2008) 281–286.
- [37] P.Z. Yujian Yao, Chao Jiang, Ryan M. DuChanois, Xuan Zhang, Menachem Elimelech, High performance polyester reverse osmosis desalination membrane with chlorine resistance, nature sustainability, 4 (2021) 138–146.
- [38] J. Zhu, F. Pan, M. Wang, Z. Zhu, J. Xiao, L. Shao, Y. Du, Z. Jiang, In-situ construction of water capture layer through reaction enhanced surface segregation for pervaporation desalination, *Journal of Membrane Science*, 658, 2022.
- [39] H. Zeng, S. Liu, J. Wang, Y. Li, L. Zhu, M. Xu, C. Wang, Hydrophilic SPEEK/PES composite membrane for pervaporation desalination, *Separation and Purification Technology*, 250, 2020.
- [40] Q. Wang, N. Li, B. Bolto, M. Hoang, Z. Xie, Desalination by pervaporation: A review, *Desalination* 387 (2016) 46–60.
- [41] D.A. Reino Olegário da Silva, L.C. Bosmuler Zuge, A. de Paula Scheer, Preparation and characterization of a novel green silica/PVA membrane for water desalination by pervaporation, *Separation and Purification Technology*, 247 (2020).
- [42] Z. Wang, J. Sun, N. Li, Y. Qin, X. Qian, Z. Xie, Tuning interlayer structure to construct steady dual-crosslinked graphene oxide membranes for desalination of hypersaline brine via pervaporation, *Separation and Purification Technology*, 286, 2022.
- [43] X. Qian, N. Li, Q. Wang, S. Ji, Chitosan/graphene oxide mixed matrix membrane with enhanced water permeability for high-salinity water desalination by pervaporation, *Desalination* 438 (2018) 83–96.
- [44] L. Li, J. Hou, V. Chen, Pinning Down the Water Transport Mechanism in Graphene Oxide Pervaporation Desalination Membranes, *Ind. Eng. Chem. Res.* 58 (2019) 4231–4239.
- [45] Y. Qian, X. Zhang, C. Liu, C. Zhou, A. Huang, Tuning interlayer spacing of graphene oxide membranes with enhanced desalination performance, *Desalination* 460 (2019) 56–63.
- [46] A. Huang, B. Feng, Synthesis of novel graphene oxide-polyimide hollow fiber membranes for seawater desalination, *J. Membr. Sci.* 548 (2018) 59–65.
- [47] X. Zhan, Z. Gao, R. Ge, J. Lu, J. Li, X. Wan, Rigid POSS intercalated graphene oxide membranes with hydrophilic/hydrophobic heterostructure for efficient pervaporation desalination, *Desalination*, 543, 2022.
- [48] W. Cha-umpong, M. Mayyas, A. Razmjou, V. Chen, Modification of GO-based pervaporation membranes to improve stability in oscillating temperature operation, *Desalination*, 516, 2021.
- [49] G. Liu, J. Shen, Q. Liu, G. Liu, J. Xiong, J. Yang, W. Jin, Ultrathin two-dimensional MXene membrane for pervaporation desalination, *J. Membr. Sci.* 548 (2018) 548–558.
- [50] G. Yang, Z. Xie, A.W. Thornton, C.M. Doherty, M. Ding, H. Xu, M. Cran, D. Ng, S. Gray, Ultrathin poly(vinyl alcohol)/MXene nanofilm composite membrane with facile intrusion-free construction for pervaporative separations, *Journal of Membrane Science*, 614, 2020.
- [51] G. Yang, Z. Xie, M. Cran, D. Ng, S. Gray, Enhanced desalination performance of poly(vinyl alcohol)/carbon nanotube composite pervaporation membranes via interfacial engineering, *J. Membr. Sci.* 579 (2019) 40–51.
- [52] G. Yang, Z. Xie, S. Zhang, H. Zheng, K. Cai, M. Cran, D. Ng, C. Wu, S. Gray, Functionalized Carbon Nanotube-Mediated Transport in Membranes Containing Fixed-Site Carriers for Fast Pervaporation Desalination, *ACS Appl. Mater. Interfaces* 12 (2020) 50918–50928.
- [53] Y. Liu, Z. Tong, H. Zhu, X. Zhao, J. Du, B. Zhang, Polyamide composite membranes sandwiched with modified carbon nanotubes for high throughput pervaporation desalination of hypersaline solutions, *J. Membr. Sci.* 641 (2022) 119889.
- [54] Y. Xing, Y. Xue, D. Qin, P. Zhao, P. Li, Microwave-Induced Ultrafast Crosslinking of Poly(vinyl alcohol) Blended with Nanoparticles as Wave Absorber for Pervaporation Desalination, *Journal of Membrane Science Letters* 100021 (2022).
- [55] J. Meng, P. Zhao, B. Cao, C.H. Lau, Y. Xue, R. Zhang, P. Li, Fabricating thin-film composite membranes for pervaporation desalination via photo-crosslinking, *Desalination* 512 (2021) 115128.
- [56] J. Wang, B. Cao, R. Zhang, P. Li, Spray-coated tough thin film composite membrane for pervaporation desalination, *Chem. Eng. Res. Des.* 179 (2022) 493–501.
- [57] S. Zachariah, Y.-L. Liu, Surface engineering through biomimicked structures and deprotonation of poly(vinyl alcohol) membranes for pervaporation desalination, *J. Membr. Sci.* 637 (2021) 119670.
- [58] P. Zhao, J. Meng, R. Zhang, B. Cao, P. Li, Molecular design of chlorine-resistant polymer for pervaporation desalination, *Sep. Purif. Technol.* 268 (2021) 118671.
- [59] D. Qin, H. Liu, T. Xiong, J. Wang, R. Zhang, B. Cao, P. Li, Enhancing the property of composite pervaporation desalination membrane by fabricating a less resistance substrate with porous but skinless surface structure, *Desalination* 525 (2022) 115496.
- [60] P. Zhao, B. Yao, J. Meng, R. Zhang, B. Cao, P. Li, Studies on the fouling behavior and cleaning method of pervaporation desalination membranes for reclamation of reverse osmosis concentrated water, *Sep. Purif. Technol.* 274 (2021) 119034.
- [61] H. Fareed, G.H. Qasim, J. Jang, W. Lee, S. Han, I.S. Kim, Brine desalination via pervaporation using kaolin-intercalated hydrolyzed polyacrylonitrile membranes, *Sep. Purif. Technol.* 281 (2022) 119874.
- [62] D. Qin, R. Zhang, B. Cao, P. Li, Fabrication of high-performance composite membranes based on hierarchically structured electrospun nanofiber substrates for pervaporation desalination, *J. Membr. Sci.* 638 (2021) 119672.
- [63] H. Liu, J. Xia, K. Cui, J. Meng, R. Zhang, B. Cao, P. Li, Fabrication of high-performance pervaporation membrane for sulfuric acid recovery via interfacial polymerization, *Journal of Membrane Science*, 624, 2021.
- [64] E. Halakoo, X. Feng, Layer-by-layer assembly of polyethyleneimine/graphene oxide membranes for desalination of high-salinity water via pervaporation, *Sep. Purif. Technol.* 234 (2020) 116077.
- [65] I. Prihatiningtyas, G.A. Gebreslase, B. Van der Bruggen, Incorporation of Al₂O₃ into cellulose triacetate membranes to enhance the performance of pervaporation for desalination of hypersaline solutions, *Desalination* 474 (2020) 114198.
- [66] I. Prihatiningtyas, Y. Li, Y. Hartanto, A. Vananroye, N. Coenen, B. Van der Bruggen, Effect of solvent on the morphology and performance of cellulose triacetate membrane/cellulose nanocrystal nanocomposite pervaporation desalination membranes, *Chem. Eng. J.* 388 (2020) 124216.
- [67] I. Prihatiningtyas, Y. Hartanto, M.S.R. Ballesteros, B. Van der Bruggen, Cellulose triacetate/LUDOX-SiO₂ nanocomposite for synthesis of pervaporation desalination membranes, *J. Appl. Polym. Sci.* 138 (2021) 50000.
- [68] D. Qin, R. Zhang, B. Cao, P. Li, Fabrication of high-performance composite membranes based on hierarchically structured electrospun nanofiber substrates for pervaporation desalination, *Journal of Membrane Science*, 638, 2021.
- [69] R. Naim, I. Levitsky, V. Gitis, Surfactant cleaning of UF membranes fouled by proteins, *Sep. Purif. Technol.* 94 (2012) 39–43.
- [70] M. Liu, Q. Chen, L. Wang, S. Yu, C. Gao, Improving fouling resistance and chlorine stability of aromatic polyamide thin-film composite RO membrane by surface grafting of poly(vinyl alcohol) (PVA), *Desalination* 367 (2015) 11–20.
- [71] S. Bano, A. Mahmood, S.J. Kim, K.-H. Lee, Chlorine resistant binary complexed NaAlg/PVA composite membrane for nanofiltration, *Sep. Purif. Technol.* 137 (2014) 21–27.
- [72] W. Yan, L. Liu, C. Dong, S. Xie, X. Zhao, C. Gao, Surface modification of reverse osmosis membrane with tannic acid for improving chlorine resistance, *Desalination*, 498, 2021.
- [73] Y. Yao, P. Zhang, C. Jiang, R.M. DuChanois, X. Zhang, M. Elimelech, High performance polyester reverse osmosis desalination membrane with chlorine resistance, *Nature Sustainability* 4 (2021) 138–146.
- [74] X. Zhang, H. Huang, X. Li, J. Wang, Y. Wei, H. Zhang, Bioinspired chlorine-resistant tailoring for polyamide reverse osmosis membrane based on tandem oxidation of natural α -lipoic acid on the surface, *Journal of Membrane Science*, 618, 2021.
- [75] Y. Yao, W. Zhang, Y. Du, M. Li, L. Wang, X. Zhang, Toward Enhancing the Chlorine Resistance of Reverse Osmosis Membranes: An Effective Strategy via an End-capping Technology, *Environ. Sci. Technol.* 53 (2019) 1296–1304.
- [76] J. Wang, S.-L. Li, Y. Guan, C. Zhu, G. Gong, Y. Hu, Novel RO membranes fabricated by grafting sulfonamide group: Improving water permeability, fouling resistance and chlorine resistant performance, *Journal of Membrane Science*, 641, 2022.
- [77] Y. Zhao, L. Dai, Q. Zhang, S. Zhou, S. Zhang, Chlorine-resistant sulfochlorinated and sulfonated polysulfone for reverse osmosis membranes by coating method, *J. Colloid Interface Sci.* 541 (2019) 434–443.
- [78] Y. He, Y. Zhang, F. Liang, Y. Zhu, J. Jin, Chlorine resistant polyamide desalination membrane prepared via organic-organic interfacial polymerization, *Journal of Membrane Science*, 672, 2023.
- [79] R. Verbeke, D.M. Davenport, T. Stassin, S. Eyley, M. Dickmann, A.J. Cruz, P. Dara, C.L. Riitt, C. Bogaerts, W. Egger, R. Ameloot, J. Meerschaert, W. Thielemans, G. Koekelberghs, M. Elimelech, I.F.J. Vankelecom, Chlorine-Resistant Epoxide-Based Membranes for Sustainable Water Desalination, *Environ. Sci. Technol. Lett.* 8 (2021) 818–824.
- [80] G. Kong, G. Yang, P. Xu, Z. Kang, H. Guo, M. Sun, Z. Yan, S. Mintova, D. Sun, Interfacial assembling of flexible silica membranes with high chlorine resistance for dye separation, *J. Membr. Sci.* 677 (2023) 121628.